pagepress

Geospatial Health 2022; volume 17(s1):1065

Spatial epidemiology and meteorological risk factors of COVID-19 in Fars Province, Iran

Marjan Zare,[1] Ali Semati,[2] Alireza Mirahmadizadeh,[2] Abdulrasool Hemmati,[2] Mostafa Ebrahimi[3]

[1]Maternal-fetal medicine Research Centre, Shiraz University of Medical Sciences; [2]Non-communicable diseases Research Centre, Shiraz University of Medical Sciences; [3]Communicable Disease Control Centre, Shiraz University of Medical Sciences, Shiraz, Iran

Abstract

This study aimed at detecting space-time clusters of COVID-19 cases in Fars Province, Iran and at investigating their potential association with meteorological factors, such as temperature, precipitation and wind velocity. Time-series data including 53,554 infected people recorded in 26 cities from 18 February to 30 September 2020 together with 5876 meteorological records were subjected to the analysis. Applying a significance level of P<0.05, the analysis of space-time distribution of COVID-19 resulted in nine significant outbreaks within the study period. The most likely cluster occurred from 27 March to 13 July 2020 and contained 11% of the total cases with eight additional, secondary clusters. We found that the COVID-19 incidence rate was affected by high temperature (OR=1.64; 95% CI: 1.44-1.87), while precipitation and wind velocity had less effect (OR=0.84; 95% CI: 0.75-0.89 and OR=0.27; 95% CI: 0.14-0.51), respectively.

Correspondence: Ali Semati, Central building of Shiraz University of Medical Sciences, Vice Chancellor for Health, fourth floor, Zand St, Shiraz, Iran.
Tel.: +98.07132122368 - Fax: +98.07132356996.
E-mail: semati.epid77@gmail.com

Key words: COVID-19; meteorology; space-time outbreaks; Iran.

Acknowledgements: the authors would like to thank Ms. A. Keivanshekouh at the Research Consultation Centre (RCC) of Shiraz University of Medical Sciences for improving the use of English in the manuscript.

Conflict of interest: the authors declare no potential conflict of interest.

Ethical statement: all ethical steps including data collection and analysis as well as reporting the results were in accordance with the standards approved by the Ethic Committee of the Ministry of Health, Treatment, and Medical Education (IR.SUMS.REC.1399.574). The work processes were anonymous and the results were reported to the study participants.

Received for publication: 25 December 2021.
Revision received: 16 April 2022.
Accepted for publication: 19 April 2022.

Geospatial Health 2022; 17(s1):1065
doi:10.4081/gh.2022.1065

Introduction

World Health Organization (WHO) is strengthening the surveillance systems for infectious diseases and developing new techniques that can prioritize times and locations for targeting interventions and resource allocations (Zare *et al*., 2019a). In January 2020, WHO declared the corona-virus disease 2019 (COVID-19) a serious epidemic (Kasraeian *et al*., 2020) and in March 2020 a pandemic. This infection is caused by the SARS-CoV-2 virus, which is the third zoonotic corona-virus breakout with human-to-human transmission in the 21st century (Xie and Chen, 2020). As it is a respiratory viral disease, COVID-19 could potentially be influenced by climatic features, such as temperature, precipitation and wind velocity (Carlson *et al*., 2020). Various studies have been done nationwide evaluating the impact of these climate variables on COVID-19 cases; however, there are still controversies on the major consequences of these factors on COVID-19 occurrence. In a review study assessing the intricate relationships between meteorological factors and COVID-19 cases, it was demonstrated that temperature as well as wind velocity and precipitation could have positive, negative or neutral effects on COVID-19 cases in different countries (Srivastava, 2021). Spatial technologies, such as geographic information systems (GIS) and spatial and temporal scan statistics (SaTScan) (Kulldorff, 2015) have assisted health managers and policymakers by detecting space-time clusters of diseases (Zare *et al*., 2019a). This study aimed at detecting space-time clusters of COVID-19 and also at investigating the associations of COVID-19 incidence rates with temperature, precipitation and wind velocity.

Materials and methods

Study design, sample size, data collection and variable definition

Time-series data, including 53,554 COVID-19 cases recorded in 26 cities of Fars Province, Iran from February 18 to September

30, 2020, were used to assess the space-time features of COVID-19. All cases registered during this period at 44 COVID-19 testing centres affiliated with Shiraz University of Medical Science were entered into the study. There were no exclusion criteria.

The COVID-19 incidence was taken as that presented by the positive cases confirmed by real-time reverse transcription polymerase chain reaction (RT-PCR). Temperature (°C), precipitation (%) and wind velocity (m/s) were measured as daily averages during each day. Information about meteorological factors was obtained from the Meteorological Organization of Fars Province. Besides, population densities were gained from the 2016 census performed in Iran, while the geographical coordinates of the locations were obtained through Google-Earth (US Dept. of State Geographer, 2021) based on the latitude-longitude coordinate system.

Study area

Fars Province, which is located in Iran at 27°3' and 31°40' northern latitude and 50°36' and 55°35' western longitude, has an area of 122.66 km^2 and a population of 4,299,676. It includes 26 cities with Shiraz as capital. The province has moderate winters with an annual rainfall of 100-600 mm. Topographically, there are three in the area including mountainous areas in the North, Northwest and West with cold winters and annual rainfalls of 400-600 mm; the central parts with mild winters and warm summers and annual rainfalls of 200-400 mm; and the southern and south-eastern parts with hot and dry summers and annual rainfalls of 100-200 mm (Zare *et al*., 2019a). This results in six specific climatic regions.

Statistical analysis

Kolmogorov-Smirnov test

To test if the data follow a given distribution, the Kolmogorov-Smirnov (KS) normality test (with the null hypothesis of normal distribution) was employed. Median (Q1, Q3) and frequency (*i.e.* relative frequency) were used to describe the non-normal quantitative and qualitative variables. The other applied statistical tests were the following.

Spearman's correlation coefficient

Correlation is defined as a relation existing between two variables which tend to vary, be associated with or occur together in a way not expected by chance alone. For non-normal distributions (presence of extreme values or outliers) the correlation coefficient is calculated from ranks of data, not from their actual values. The coefficient designed for this purpose, ρ (Akoglu, 2018) is described as:

$$\rho = 1 - \frac{6\sum d_i^2}{n(n^2-1)} \quad (1)$$

where d_i is the difference between the two ranks of observations; and n the number of observations.

Generalized linear model

Generalized linear models are used to analyse data following non-normal distributions. It works by obtaining maximum likelihood estimates of the parameters with observations distributed according to some exponential family and systematic effects that can be made linear by a suitable transformation or link function. A generalization of the analysis of variance is given for these models using log-likelihoods (Nelder and Wedderburn, 1972). In this context, the Poisson regression, described by equation 2 below, models how the mean of a discrete (count) response variable Y depends on a vector of explanatory variables x:

$$\log \lambda = \alpha + \beta x \quad (2)$$

where log is the natural logarithm (to the base of e=2.7); λ the mean of Poisson distribution (E(Y|x)); α the intercept; and β the coefficient of the regression line.

Random component: the distribution of Y is Poisson with mean λ.

Systematic component: x is the explanatory variable (can be continuous or discrete) and is linear in the parameters. This can be extended to multiple variables of non-linear transformations.

Link function: the log link function is used:

$$\text{Odds ratio (OR)} = \exp(\beta) \quad (3)$$

Space-time scan statistics and clusters within a cluster methodology

Space-time permutation modelling, with which permutation scan statistics is derived, was used to detect high-rate clusters considering time aggregation unit =day, time aggregation length =one day, minimum temporal cluster size =1 day; maximum temporal cluster size =50% of the study period; minimum cases for high rates =2; maximum spatial cluster size =50% of the population at risk; and the number of replications =999. Temporal data were checked to ensure that all cases were within the specified temporal study period. In addition, geographical data check was done to

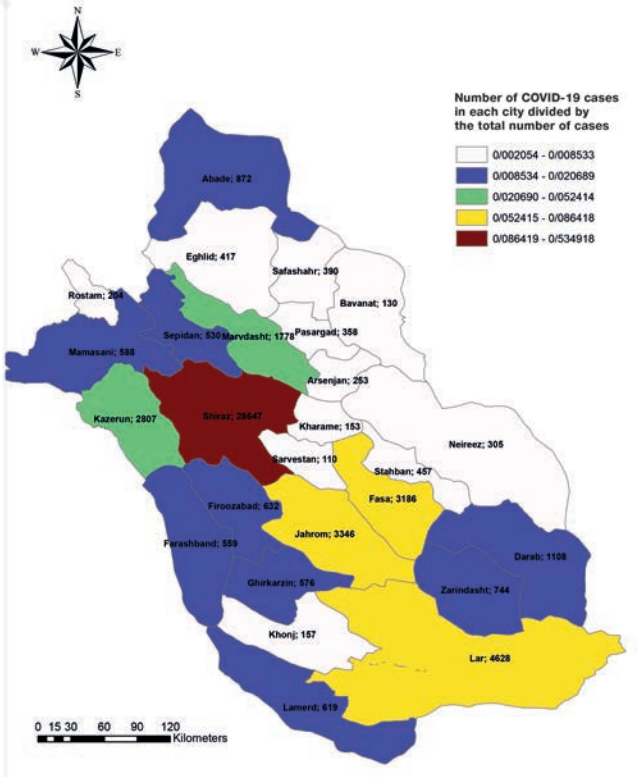

Figure 1. The geographical distribution of the total 53,554 COVID-19 cases in the 26 cities of Fars province, Iran during October 1–November 14, 2020.

ensure that all observations were within the specified geographical area. No geographical overlap as criterion for clusters and sub-group analysis were used. Here permutation scan statistics tested the null hypothesize of constant risk over space and time. Permutation scan statistics can be visualized as a cylinder based on a window (here circular) that moves across space using an adjustable diameter that can vary from zero to maximum, *e.g.*, a city. The cylinder height is the time period and whenever and wherever the observed number of cases exceeds the expected number of cases, a cluster (characterized by the log likelihood ratio), is reported (Kulldorff, 2015). When a detected cluster is large, it may be interesting to look for clusters within that cluster in the same way (Zare *et al*., 2017, 2019a).

ArcGIS, version 10 (https://help.arcgis.com/en/arcgisdesktop/10.0/), R version 3.6.3 (https://www.r-project.org/) and SaTScan software (https://www.satscan.org/) were applied. A significance level of 0.05 was considered for all tests.

Results

Geographical distribution of COVID-19

The geographical distribution of the total 53,554 COVID-19 cases recorded in the 26 cities of Fars Province from February 18 to September 30, 2020 is depicted in Figure 1. The largest number of cases (53.49%) occurred in Shiraz followed by Lar (8.64%), Jahrom (6.25%) and Fasa (5.95%), while the lowest numbers occurred in Sarvestan (0.20%) followed by Bavanat (0.24%) and

Table 1. The association between incidence rates of COVID-19 and key climate variables in Fars Province, Iran February 18-September 30, 2020.

Variable	Median (Q1, Q3)	ρ	P-value	OR	95% CI
Temperature (°C)	24.36 (20, 30)	0.21	<0.001	1.64	1.44-1.87
Precipitation (%)	31.50 (22, 40.50)	–0.07	<0.001	0.84	0.75-0.89
Wind velocity (m/s)	2.31 (2, 3)	–0.09	<0.001	0.27	0.14-0.51

Q1, first quartile; Q2, third quartile; ρ, Spearman's correlation coefficient; OR, odds ratio; CI, confidence interval.

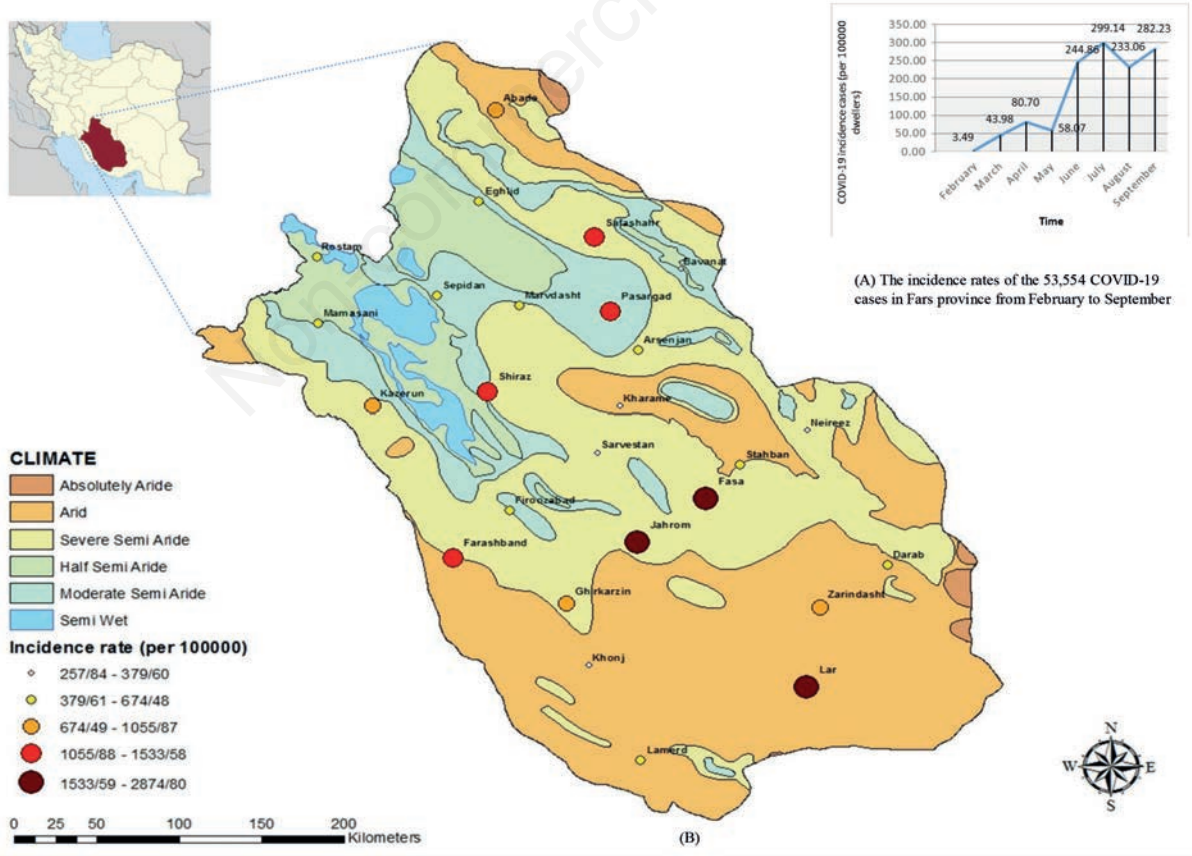

Figure 2. The time distribution of COVID-19 incidence rates from 18 February to 30 September 2020 (A) and climatic distribution of COVID-19 incidence rates by 26 cities and six climate zones (B).

Kharame (0.28%). It should be noted that the COVID-19 cases were not distributed uniformly across the cities (test statistics =1391.66, df =25, P<0.001) where df is the degree of freedom.

Time distribution of COVID-19

Out of the total COVID-19 cases, 0.3% occurred in February, 3.5% in March, 6.5% in April, 4.7%in May, 19.7%in June, 24.0% in July, 18.7% in August, and 22.6 % in September. It should be mentioned that the COVID-19 cases were not distributed uniformly across the months (test statistics =520.36, df=7, P<0.001). In addition, an increasing trend was observed incidence rates from February to September (Figure 2A). There was also COVID-19 one peak in each season; April in spring and July in summer.

Meteorological factors and COVID-19

The association between the 5876 recorded meteorological factors and the incidence rates of the 53,554 COVID-19 cases in Fars Province during the study period are presented in Table 1.

There was a higher COVID-19 incidence rate with higher temperatures, with lower incidence rates together with higher precipitation and higher wind velocity. The incidence rates of the 53,554 COVID-19 cases in relation to the six different climates in the different areas of the province are depicted in Figure 2B.

Coldness and humidity decrease, while warmth and dryness increase when one moves from north to the south in the province. In this study, the highest COVID-19 incidence rates were detected in Lar, Jahrom and Fasa, which are located in arid and semi-arid climates.

Space-time outbreaks of COVID-19

The space-time COVID-19 outbreaks and the related subgroups are presented in Table 2. Nine statistically significant space-time outbreaks including 94% of the total cases were detected during 18 February-30 September 2020. In addition, sub cluster analysis revealed significant clusters within three large clusters.

The most likely cluster (MLC) included 11% of the total number of cases and eight secondary clusters comprised 83% of the cases during the study period (P<0.001). However, the space-time distribution of the disease in Fars Province was far from stationary. The MLC covered 77% of the cases in Lar as well as 16% of the cases that occurred in April, June and July. Moreover, 53% of the secondary cluster cases belonged to cluster 5 that included Shiraz during the period April 3-16, 2020. In fact, it included 52% of all cases that occurred in April. Furthermore, 0.59%, 0.62%, 5%, 0.63%, 1%, 0.33% and 1% of the total cases belonged to the clusters 2, 3, 4, 6, 7, 8 and 9, respectively. Only 6% of the total cases were not included in the detected outbreaks. Subgroup analysis revealed significant outbreaks covered by the MLC including Lamerd, Khonj and Ghirkarzin during July 10-13, 2020, with Ghirkarzing as the epicentre. Other cities were epicentres at different times: Lamerd on March 5 and 23 June; Khonj on September 3-27; and Ghirkarzin on June 24 and September 2; cluster 4 included three epicentres including Abade, Safashahr and Sepidan, which occurred on September 17-30; on June 9 and July 18; and during August 22-23, respectively; cluster 6 included Mamasani as epicentre during June 27-30, 2020.

Table 2. COVID-19 cluster analysis in Fars Province, Iran February 18-September 30, 2020.

Cluster	Location	Radius (km)	Epicentre	Start date	End date	Test statistic	Critical value°	P-value
MLC*	Lamerd, Khonj, Ghirkarzin, Lar	119.70	Lamerd	2020/05/27	2020/07/13	321.17	10.58	<0.001
Cluster 2	Fasa	0	Fasa	2020/09/24	2020/09/26	135.43	10.58	<0.001
Cluster 3	Jahrom	0	Jahrom	2020/09/26	2020/09/29	125.57	10.58	<0.001
Cluster 4	Abade, Eghlid, Safashahr, Bavanat, Pasargad, Sepidan	128.74	Abade	2020/08/22	2020/09/01	95.27	10.58	<0.001
Cluster 5	Shiraz	0	Shiraz	2020/04/03	2020/04/16	82.47	10.58	<0.001
Cluster 6	Kazerun, Mamasani	55.26	Kazerun	2020/07/10	2020/07/21	60.90	10.58	<0.001
Cluster 7	Farashband	0	Farashband	2020/09/21	2020/09/21	35.14	10.58	<0.001
Cluster 8	Marvdasht	0	Marvdasht	2020/06/26	2020/06/29	29.89	10.58	<0.001
Cluster 9	Firoozabad	0	Firoozabad	2020/07/11	2020/07/11	26.51	10.58	<0.001
Sub-cluster results								
MLC*	Lamerd, Khonj, Ghirkarzin	114.69	Ghirkarzin	2020/07/10	2020/07/13	63.93	7.28	<0.001
	Lamerd	0	Lamerd	2020/03/05	2020/06/23	16.70	5.18	<0.001
	Khonj	0	Khonj	2020/09/03	2020/09/27	71.48	5.18	<0.001
	Ghirkarzin	0	Ghirkarzin	2020/06/24	2020/09/02	10.20	5.18	<0.001
Cluster 4	Abade	0	Abade	2020/09/17	2020/09/30	20.32	6.90	<0.001
	Safashahr	0	Safashahr	2020/06/09	2020/07/18	96.46	6.90	<0.001
	Sepidan	0	Sepidan	2020/08/22	2020/08/23	22.20	6.90	<0.001
Cluster 6	Mamasani	0	Mamasani	2020/06/27	2020/06/30	8.01	5.45	0.002

*Most likely cluster; °Standard Monte Carlo critical value.

Discussion

In our hands, permutation scan statistics detected space-time outbreaks effectively, which is in accordance with work using this approach in other countries. For example, in the United States, space-time outbreaks of COVID-19 were detected by Desjardins *et al*. (2020) during two periods and in Hong Kong, Kan *et al*. (2021) similar results. Furthermore, it has been shown that space-time permutation scan statistics works well for the detection of frequent outbreaks of many infectious diseases (Zare *et al*., 2017, 2019b; Rezaianzadeh *et al*., 2018; Rezaianzadeh *et al*., 2020) .

Climatically, we found higher COVID-19 incidence rates in higher temperatures, while fewer incidence rates were seen in conditions involving higher precipitation and stronger wind velocity. The average temperature was also positively correlated to similar COVID-19 trends in Jakarta, China and India (Pawar *et al*., 2020; Tosepu *et al*., 2020; Xie and Zhu, 2020). However, some studies have reported negative associations in this regard (Shi *et al*., 2020, Rosario *et al*., 2020; Notari, 2021). On the other hand, no evidence was obtained supporting a decline in the number of COVID-19 cases in high temperatures in Brazil and China (Jamil *et al*., 2020; Prata *et al*., 2020).

Previous studies, consistent with our findings, revealed a negative correlation between the number of COVID-19 cases and humidity (Ahmadi *et al*., 2020; Haque and Rahman, 2020; Wang *et al*., 2020; Wu *et al*., 2020) and wind velocity (Ahmadi *et al*., 2020; Coccia, 2020; Rendana, 2020; Rosario *et al*., 2020). In Turkey, however, Şahin (2020) reported higher average temperatures and higher wind velocity and humidity to be reported to be negatively correlated to COVID-19; yet, due to lack of statistical significance, the results should be considered with due caution. In line with the current results, precipitation was shown to be a good predictor of COVID-19 in the United States (Gupta *et al*., 2020). However, no significant relationship was seen between lower precipitation and the number of COVID-19 cases in Spain (Briz-Redón and Serrano-Aroca, 2020).

Several limitations were encountered, which might have affected our results. Firstly, the surveillance system of infectious diseases in Iran is a passive system and many COVID-19 infected people with none, mild or moderate symptoms do not generally come to health centres and were therefore not diagnosed resulting in a probable underestimation of the reported incidence rates. This could affect the prediction of new COVID-19 cases, space-time outbreaks as well as COVID-19 loads. Secondly, like other detection methods, scan statistics could discover more than one cluster in a given area and time. Hence, interpretation of the results is sometimes difficult and so is prioritizing of clusters. Thirdly, although the detected clusters were ranked based on their likelihood-ratio scores, prioritizing statistical and clinical significance is still under debate and a scale-free statistic, such as risk attributed to populations (a value between 0 and 1) alongside statistical significance can be helpful. The other restriction of scan statistics is that the exact boundaries of the discovered clusters remain inexact. Thus, detected clusters may not reflect a high risk everywhere, while high-risk sites may exist outside the cluster. This can occur when a circular scan window is used, while the cluster shape is oval or irregular. The way to deal with this problem is either to increase the sample size or using the Oliver-F measure, which gives values between 0 and 1 for each location; the closer to 1, the more likely that the related location is part of a factual cluster. The Oliver-F measure is derived from SaTScan (Kulldorff, 2015) when the Poisson distribution (purely spatial) is used. Hyper-geometric distribution (space-time permutation scan modelling), however, was used in the current work. It is worth mentioning that sub-group analysis used to detect significant clusters could also be a solution here. Another problem that can potentially lead to a limited outcome would be lack of information on human movements and contacts, in which case one would have to explore meteorological risk factors related to COVID-19 without considering any factors directly but in some indirect way reflecting human movements and contacts. In addition, further investigations are needed regarding genetic variants of SARS-CoV-2, vaccination and drug treatment of COVID-19 as well as studies of human movements and contacts.

Conclusions

Respiratory viral infections are supposed to be positively associated with cold weather; however, the current geospatial investigation revealed a positive association between COVID-19 incidence rate and warm weather. Therefore, in order to oppose coming outbreaks of the variants of concern, such as Delta and Omicron, forecasts are required for deployment of medical equipment and resources in these areas; especially, in the warm season of the year. In addition, vaccination coverage including a third and fourth booster doses, is mandatory and must be part of a surveillance-response system.

References

Ahmadi M, Sharifi A, Dorosti S, Ghoushchi SJ, Ghanbari N, 2020. Investigation of effective climatology parameters on COVID-19 outbreak in Iran. Sci Total Environ 729:138705.

Akoglu H, 2018. User's guide to correlation coefficients. Turk J Emerg Med 18:91-93.

Briz-Redón Á, Serrano-Aroca Á, 2020. A spatio-temporal analysis for exploring the effect of temperature on COVID-19 early evolution in Spain. Sci Total Environ 728:138811.

Carlson CJ, Gomez AC, Bansal S, Ryan, SJ, 2020. Misconceptions about weather and seasonality must not misguide COVID-19 response. Nat Commun 11:1-4.

Coccia M, 2020. How do low wind speeds and high levels of air pollution support the spread of COVID-19? Atmos Pollut Res 12:437-45.

Desjardins M, Hohl A, Delmelle E, 2020. Rapid surveillance of COVID-19 in the United States using a prospective space-time scan statistic: detecting and evaluating emerging clusters. Appl Geogr 118:102202.

Gupta S, Raghuwanshi GS, Chanda A, 2020. Effect of weather on COVID-19 spread in the US: A prediction model for India in 2020. Sci Total Environ 728:138860.

Haque SE, Rahman M, 2020. Association between temperature, humidity, and COVID-19 outbreaks in Bangladesh. Environ Sci Policy 114:253-5.

Jamil T, Alam I, Gojobori T, Duarte CM, 2020. No evidence for temperature-dependence of the COVID-19 epidemic. Front Public Health 8:436.

Kan Z, Kwan MP, Wong MS, Huang J, Liu D, 2021. Identifying the space-time patterns of COVID-19 risk and their associations with different built environment features in Hong Kong.

Sci Total Environ 772:145379.
Kasraeian M, Zare M, Vafaei H, Kasraeian M, Asadi N, 2020. COVID-19 pneumonia and pregnancy; a systematic review and meta-analysis. J Matern Fetal Neonatal Med 1-8.
Kulldorff M, 2015. SaTScan - software for the spatial, temporal, and space-time scan statistics. 2016. Boston: Harvard Medical School and Harvard Pilgrim Health Care. Available from http:www.satscan.org
Nelder JA,Wedderburn RW, 1972. Generalized linear models. J R Stat Soc Ser A Stat Soc 135:370-84.
Notari A, 2021. Temperature dependence of COVID-19 transmission. Sci Total Environ 763:144390.
Pawar S, Stanam A, Chaudhari M, Rayudu D, 2020. Effects of temperature on COVID-19 transmission. Medrxiv.
Prata DN, Rodrigues W, Bermejo PH, 2020. Temperature significantly changes COVID-19 transmission in (sub) tropical cities of Brazil. Sci Total Environ 729:138862.
Rendana M, 2020. Impact of the wind conditions on COVID-19 pandemic: A new insight for direction of the spread of the virus. Urban Clim 34:100680.
Rezaianzadeh A, Zare M, Aliakbarpoor M, Faramarzi H, Ebrahimi M, 2020. Space-Time Cluster Analysis of Malaria in Fars Province-Iran. Int. J Infect 7:e107238.
Rezaianzadeh A, Zare M, Tabatabaee H, Ali-Akbarpour M, Faramarzi H, Ebrahimi M, 2018. Does prospective permutation scan statistics work well with cutaneous leishmaniais as a high-frequency or malaria as a low-frequency infection in Fars province, Iran? Asian Pac J Trop Biomed 8:478-484.
Rosario DK, Mutz YS, Bernardes PC, Conte-Junior CA, 2020. Relationship between COVID-19 and weather: Case study in a tropical country. Int J Hyg Environ Health 229:113587.
Şahin M, 2020. Impact of weather on COVID-19 pandemic in Turkey. Sci Total Environ 728:138810.
Shi P, Dong Y, Yan H, Zhao C, Li XY, Liu W, He M, Tang SX, Xi SH, 2020. Impact of temperature on the dynamics of the COVID-19 outbreak in China. Sci Total Environ 728:138890.
Srivastava A, 2021. COVID-19 and air pollution and meteorology-an intricate relationship: a review. Chemosphere 263:128297.
Tosepu R, Gunawan J, Effendy DS, Ahmad OAI, Lestari H, Bahar H, Asfian P, 2020. Correlation between weather and Covid-19 pandemic in Jakarta, Indonesia. Sci Total Environ 725:138436.
Wang J, Tang K, Feng K, Lin X, Weifeng L, Chen K, Wang F, 2020. High temperature and high humidity reduce the transmission of COVID-19. Available from: https://ssrn.com/abstract=3551767 2020
WHO, 2020. Director-General's opening remarks at the media briefing on COVID-19-11 March 2020. Available from: https://www.who.int/director-general/speeches/detail/who-director-general-s-opening-remarks-at-the-media-briefing-on-covid-19—-11-march-2020 Accessed: 10 April 2020.
Wu Y, Jing W, Liu J, Ma Q, Yuan J, Wang YP, Du M, Liu M, 2020. Effects of temperature and humidity on the daily new cases and new deaths of COVID-19 in 166 countries. Sci Total Environ 729:139051.
Xie J, Zhu Y. 2020. Association between ambient temperature and COVID-19 infection in 122 cities from China. Sci Total Environ 724:138201.
Xie M, Chen Q, 2020. Insight into 2019 novel coronavirus - An updated interim review and lessons from SARS-CoV and MERS-CoV. Int J Infect Dis 94:119-24.
Zare M, Rezaianzadeh A, Tabatabaee H, Mohsen A, Faramarzi H, Ebrahimi M, 2017. Spatiotemporal clustering of cutaneous leishmaniasis in Fars province, Iran. Asian Pac J Trop Biomed 7:862-9.
Zare M, Rezaianzadeh A, Tabatabaee H, Faramarzi H, Mohsen A, Ebrahimi M, 2019a. Determining endemic values of cutaneous leishmaniasis in Iranian Fars province by retrospectively detected clusters and receiver operating characteristic curve analysis. Asian Pac J Trop Biomed 9:359-64.
Zare M, Rezaianzadeh A, Tabatabaee H, Faramarzi H, Mohsen A, Ebrahimi M, 2019b. Establishment of an early warning system for cutaneous leishmaniasis in Fars province, Iran. Asian Pac J Trop Biomed 9:232-9.